Materials Today Nano 16 (2021) 100138

Contents lists available at ScienceDirect

Materials Today Nano

journal homepage: https://www.evise.com/profile/#/MTNANO/login

Encapsulating FeCo alloys by single layer graphene to enhance microwave absorption performance

X.J. Cui [a, b, c, e], Q.R. Jiang [a, e], C.S. Wang [d], S.H. Wang [a], Z.Y. Jiang [a, **], X.A. Li [d, ***], D.H. Deng [a, b, c, *]

[a] State Key Laboratory of Physical Chemistry of Solid Surfaces, Collaborative Innovation Center of Chemistry for Energy Materials, College of Chemistry and Chemical Engineering, Xiamen University, Xiamen, 361005, Fujian, PR China
[b] State Key Laboratory of Catalysis, Collaborative Innovation Center of Chemistry for Energy Materials, Dalian Institute of Chemical Physics, Chinese Academy of Sciences, Dalian, 116023, Liaoning, PR China
[c] University of Chinese Academy of Sciences, Beijing, 100049, PR China
[d] College of Environment and Chemical Engineering, Yanshan University, Qinhuangdao, 066004, Hebei, PR China

ARTICLE INFO

Article history:
Received 25 June 2021
Received in revised form
12 August 2021
Accepted 25 August 2021
Available online 6 September 2021

Keywords:
FeCo alloy
Single layer graphene
Core–shell structures
Numerical simulation
Microwave absorption
Enhancement mechanism

ABSTRACT

Graphene/magnetic metal hybrid nanostructures are promising candidates of novel microwave absorption materials. Although many efforts have been devoted to fabricate various graphene/magnetic metal hybrid composites, the microwave absorption performance of these materials is still far from industrial demand due to the not well balance between electric field and magnetic field characteristics. Herein, we report single layer graphene encapsulating FeCo alloy nanoparticles (FeCo@Cs) with excellent microwave absorption performance, which deliver a reflection loss value exceeding −10 dB in the whole Ku-band, whole X-band, whole C2-band, and even in the whole C1-band by varying the absorber thickness. The control experiments and numerical simulations demonstrate that the introduction of graphene coating on FeCo alloy nanoparticles can improve the microwave absorption performance greatly by increasing the electrical loss. Moreover, decreasing the coating thickness to single layer graphene can render a good match between electric field and magnetic field, and thus resulting in an electrifying microwave absorption performance. This work gives new insights into the absorption enhancement of graphene/magnetic metal hybrid structures and contributes to guide the design and development of highly efficient microwave absorption materials for practical application.

© 2021 Elsevier Ltd. All rights reserved.

1. Introduction

With the rapid rise in communication technology, high-power electronic instruments, and new style radar, it is essential to develop high-performance microwave absorption materials with strong absorption ability, broad absorption bandwidth, and high stability to eliminate adverse microwaves effectively in healthcare, electronic safety, and national defense security [1–20]. Graphene/magnetic metal hybrid nanostructures become popular candidates of novel microwave absorption materials due to their excellent ferromagnetic resonance properties, which may improve the impedance matching and broaden absorption bandwidth [21–25]. Therefore, tremendous efforts have been devoted to construct various graphene/magnetic metal composites, such as magnetic metal nanoparticles growing on graphene surfaces [26–30] and magnetic metal@multilayer graphene core@shell structures [31–34]. Compared to the magnetic particles supported on the graphene surface, the core@shell structures can isolate the metal core from air and keep it from oxidation, which can efficiently enhance the absorption performance [35–39]. However, the previously reported graphene shells are mainly multilayers, and the number of layers coated on the metal core is not controllable. These lead to the complexity of the core@shell structures and degrade the absorption performance due to the reduced magnetic loss [34,40]. In addition, the mechanism of microwave absorption for magnetic metal@graphene is still far from being completely understood. Hence, it is highly desired to construct a well-defined magnetic

* Corresponding author.
** Corresponding author.
*** Corresponding author.
E-mail addresses: zyjiang@xmu.edu.cn (Z.Y. Jiang), lixueai@ysu.edu.cn (X.A. Li), dhdeng@dicp.ac.cn (D.H. Deng).
[e] These authors contributed equally to this work.

https://doi.org/10.1016/j.mtnano.2021.100138
2588-8420/© 2021 Elsevier Ltd. All rights reserved.

metal@graphene core@shell structure to improve the microwave absorption performance, which can also serve as an ideal model to investigate the mechanism of microwave absorption for magnetic metal@graphene. On the other hand, the microstructure of core@shell structures is at the nanometer scale, but the wavelength of microwave is at the order of centimeters, which leads to the eigen values of the mathematical model differing by several orders of magnitude, and the numerical solution of the model cannot be obtained. Therefore, it is also urgent to develop a numerical simulation method to overcome the great numerical gap between nanostructures and microwave wavelength to reveal insight into the microwave absorption mechanism. Herein, we propose a strategy to construct single layer graphene encapsulating FeCo alloy nanoparticles (FeCo@Cs) with excellent microwave absorption performance, which deliver a reflection loss (RL) value exceeding −10 dB in the whole Ku-band, whole X-band, whole C2-band, and even in the whole C1-band by varying the simulation thickness. More importantly, a numerical simulation method has been proposed to get a deep understanding of the absorbing performance enhancement of single layer graphene for FeCo alloy nanoparticles. The simulation results indicate that the Poynting vector increased obviously at the contact position of the FeCo@Cs spheres and the introduction of the graphene layer can improve the microwave absorption performance greatly by increasing the electrical loss. In addition, decreasing the coating thickness to single layer graphene can render a good match between electric field and magnetic field, and thus resulting in an electrifying microwave absorption performance.

2. Results and discussion

Single layer graphene encapsulating FeCo alloy nanoparticles were prepared through a chemical vapor deposition (CVD) method [41]. First, metal-containing precursors were filled into the channel of SBA-15 by an impregnation method. Then the materials were reduced to metal nanoparticles with temperature programmed from room temperature to 800 °C under 50% H_2/Ar; thereafter single layer graphene was coated on the metal nanoparticles in the channels of SBA-15 by means of CH_4 pyrolysis at 800 °C. Finally, the samples were treated in 4% hydrofluoric acid (HF) aqueous solution to remove SBA-15 and bare metal nanoparticles. As shown in Figs. 1a and S1, transmission electron microscopy (TEM) images indicate that FeCo@Cs consist of uniform spheres with the diameter in the range of 6–10 nm. The high-resolution (HR) TEM analysis further indicates that the nanospheres consist of metal nanoparticles, which are completely encapsulated by the graphene shell with layer thickness around 3.4 Å (Figs. 1b, S1). According to the statistical analysis by HRTEM (Fig. S1), most of the graphene shells (>98%) consist of only one layer. In addition, the metal nanoparticles exhibit a spacing of 2.0 Å, in line with the (110) plane of the FeCo alloy. Thus, it can be deduced that as-prepared products are FeCo nanoparticles encapsulated by the single layer graphene shell (Fig. 1c). Fig. 1d–f shows the high-angle annular dark field scanning TEM (HAADF-STEM) image and the elemental maps of the concentration of Fe and Co. Fe and Co atoms distribute homogeneously over all nanoparticles and they are completely overlapped with the STEM images, further confirming the alloy structure of FeCo. Note that the single layer graphene shells on FeCo nanoparticles by HAADF-STEM are invisible due to the much weaker contrast grade of carbon compared with Co and Fe metals. The crystal structure of FeCo alloy nanoparticles was also confirmed by X-ray diffraction (XRD) patterns (Fig. 1g), which shows characteristic peaks at 44.9°, 65.3° and 82.7°, in good agreement with the (110), (200) and (211) planes of the FeCo alloy, respectively. In addition, almost no carbon signal can be observed in the XRD patterns, which further evidences that the shells encapsulating FeCo nanoparticles are extremely thin, in consistent with the HRTEM results. Furthermore, Raman spectrum was adopted to identify the graphene shell. As shown in Fig. 1h, the Raman spectrum of the FeCo@Cs displays three bands, at 1,350 cm^{-1}, 1,580 cm^{-1} and 2,700 cm^{-1}, which correspond to the D, G, and 2D bands of graphene. The intensity ratio (I_D/I_G) is about 0.7, indicating that the graphene encapsulating FeCo alloys is with some lattice defects, which may be caused by the high curvature of graphene. Note that the shape and intensity of the second-order two-phonon mode located near 2,700 cm^{-1} has often been utilized as a 'fingerprint' to identify the number of layers in graphene materials [42]. FeCo@Cs sample exhibits a sharp and symmetric peak, which suggests a single-layer nature of the graphene sample, further confirming the HRTEM analysis. The chemical states of these nanoparticles by X-ray photoelectron spectroscopy (XPS) (Fig. 1i) suggest that both Fe and Co in FeCo@Cs maintain their metallic state, which is also consistent with the XRD analysis and HRTEM results. Combining TEM images, XRD patterns, Raman spectrum, and XPS analysis, we find that FeCo nanoparticles are completely encapsulated by the single layer graphene shell, and such a structure will avoid the oxidation or corrosion of FeCo alloy when exposed to air or humid condition.

To evaluate the microwave absorption properties of as-prepared FeCo@Cs nanostructures, the relative complex permittivity (ε_r) and the relative complex permeability (μ_r) of the FeCo@Cs-based sample were measured by a vector network analyzer in the frequency range of 2–18 GHz (Fig. S2a, and b). Then the RL values were calculated according to transmission line theory. As shown in Fig. 2a, the FeCo@Cs sample exhibits excellent microwave absorption performance, not only with high absorption capability but also with broad effective absorption bandwidth. With a thickness of 2.1 mm, the RL value can reach −32 dB at 12.8 GHz. Moreover, the effective absorption (RL < −10 dB) bandwidth can reach 8.3 GHz (9.7–18.0 GHz), covering the entire Ku bands. Usually, according to the working frequency for the electronic instruments, the microwave is divided into several bands, e.g., in the frequency of 2–18 GHz, the microwave is further divided into S band (2–4 GHz), C band (4–8 GHz), X band (8–12 GHz), and Ku band (12–18 GHz). The working frequency for communication satellites is usually in the C band, and for the digital broadcast satellites it is usually in the Ku band. Besides, different radars can be designed to work in the C, X, and Ku bands, respectively. Therefore, the effective absorption frequency of the microwave absorption materials should entirely cover one or more bands. As mentioned above, with a thickness of 2.1 mm, the RL < −10 dB can cover the whole Ku-band, while it exceeds −20 dB over the 11.8–13.9 GHz range, absorbing more than 99% of the incident microwave in the frequency range. Furthermore, with a thickness of 2.5 mm, the effective absorption bandwidth is 5.6 GHz (7.9–13.5 GHz), which can completely cover the whole X-band (8–12 GHz). When the thickness increases to 3.1 mm, the RL can reach a value of −46 dB at 7.8 GHz, and the effective absorption bandwidth is 4.2 GHz (6.0–10.2 GHz), completely covering the whole C2-band (6–8 GHz). It should be pointed out that there are few reports concerning the microwave absorption materials with effective absorption in the range of 2–6 GHz [43–46]. In the present case, with a thickness of 4.5 mm, the sample shows considerable absorption in the C1 band (4–6 GHz). The RL value of the sample is up to −33 dB at 4.9 GHz, and the RL exceeds −10 dB in the whole C1 band, which have been barely reported in the literature. These results suggest that FeCo@Cs nanostructures have great practical applied foreground in the field of microwave absorption materials.

For graphene/magnetic metal hybrid nanostructures, the magnetic property dominates the magnetic loss for the microwave

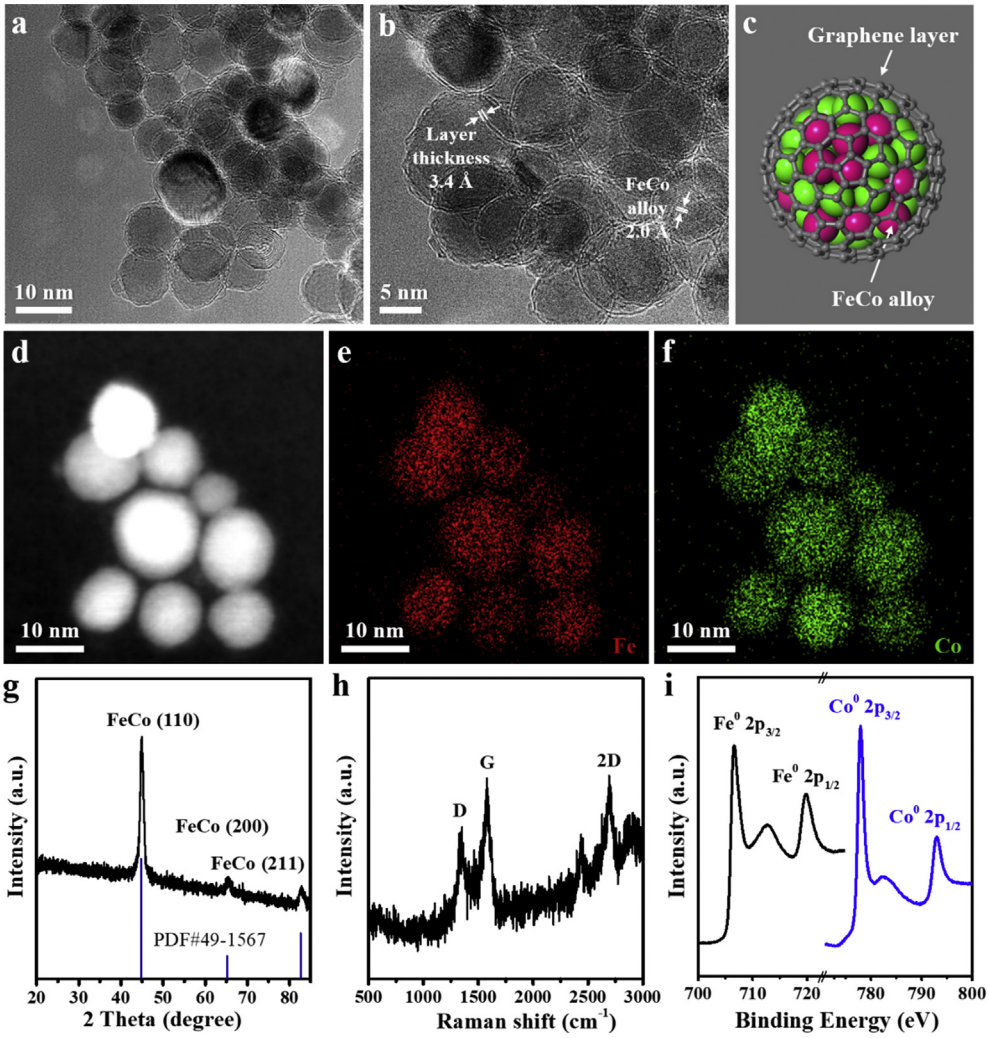

Fig. 1. Morphology and structural characterizations of FeCo@Cs. (a) Typical TEM images; (b) HRTEM images; (c) a schematic illustration of the FeCo@Cs structure; (d–f) HAADF-STEM image and corresponding energy dispersive X-ray detector (EDX) mapping images; (g) XRD patterns; (h) Raman spectrum; and (i) XPS spectra.

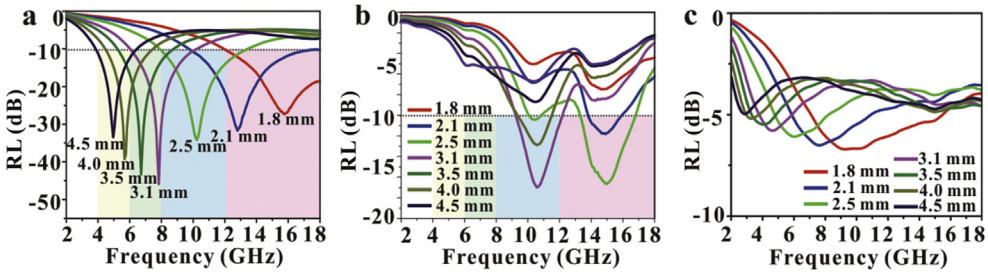

Fig. 2. The calculated reflection loss curves of the samples with the frequency from 2 to 18 GHz. (a) FeCo@Cs; (b) FeCo@oxides; and (c) FeCo alloy encapsulated by multilayer graphene.

absorption. In the present case, the unique core@shell structures ensure that the FeCo alloy particles can be protected from oxidative corrosion by the graphene, which endows the FeCo@Cs with typical ferromagnetic characteristics. The FeCo@Cs sample presents a strong saturation magnetization (*Ms*, 156 emu/g) and a low intrinsic coercivity (*Hc*, 43 Oe) (Fig. S3). The higher *Ms* and lower *Hc* are favorable to the improvement of the initial permeability, which usually indicates a strong magnetic loss ability [47,48]. In contrast, without graphene cages, FeCo nanoparticles prepared in the channels of mesoporous silica (SBA-15) were easily oxidized in the surface and formed FeCo@oxides nanostructures (Fig. S4), and the FeCo@oxides sample only shows ordinary microwave absorption properties with an effective absorption bandwidth of 3.6 GHz (Fig. 2b). In addition, the FeCo oxides encapsulated by the cracked graphene cages and supported on the graphene were prepared, respectively (Fig. S5–S7). Their poor microwave absorption performance further evidences the advantage of intact graphene encapsulating metallic FeCo alloy nanoparticles. It should also be

pointed out that, too thick graphene shell will also weaken the magnetic loss ability and the microwave absorption performances (Fig. S8, Fig. 2c). Moreover, compared to the representative magnetic materials/graphene composites, FeCo@Cs exhibited much better microwave absorption performance (Table S1) [10–13,19,23,24,35,38,39,49–53]. Thus, the unique structure of single layer graphene encapsulating metallic FeCo alloy nanoparticles, the proper thickness of graphene layer, and suitable chemical components could well balance the magnetic loss and dielectric loss, and effectively improve the microwave absorption performance, especially broad bandwidth response.

To further get insights into the microwave absorption enhancement of as-prepared FeCo@Cs, a numerical model was built in the software of COMSOL to investigate the microwave absorption process. The stable arrangement of spheres is shown in Fig. 3a, and a rectangular simulation domain with Floquet-periodic boundary conditions is carried out to express the array of the spheres in Fig. 3a [54]. A transverse electromagnetic wave with a power of 1 W is excited from the source port and injected into the spherical array. Perfectly matched layers (PMLs) on the top and bottom of the computational domain are used to absorb the reflected and transmitted electromagnetic waves respectively. Considering the amount of numerical calculation and the accuracy of numerical results, the particle radius is set to 30 μm with the composition ratio unchanged and the number of particle layers is 40. The selection method of electromagnetic parameters for the metal particle core and graphene coating is described in detail in the Supporting information.

The electromagnetic field in the simulation domain is obtained by solving Maxwell equations in the frequency domain. Based on the simulated results, the absorption characteristics of the composite material with different thicknesses are shown in Fig. 3b. Similar to the measured FeCo@Cs sample, the simulation sample also shows excellent absorption properties, especially the absorption bandwidth. With the thickness of 1.9 mm, the simulated effective absorption bandwidth of the FeCo@Cs structure with single graphene layer is 7.7 GHz (10.3–18.0 GHz), which can completely cover the whole Ku band. When the thickness increases to 2.5, 3.1, and 4.1 mm, the effective absorption bandwidths are 5.9 GHz (7.2–13.1 GHz), 4.5 GHz (5.5–10 GHz), and 2.7 GHz (4.0–6.7 GHz), respectively, which can completely cover the whole X band, C2 band, and C1 band. Except for some slight differences in specific values, the absorption bandwidths and their trends are in good agreement with the measured FeCo@Cs samples in experiments. Compared with FeCo alloy encapsulated by multilayer graphene (Fig. 3c), the microwave absorption performance of FeCo@Cs sample is much better. With the same simulation thickness, the simulated efficient absorption bandwidth narrows obviously when the graphene layer increases from single layer to multilayer, and the trend is also similar to the experimental results.

In order to further analyze the absorbing mechanism of the composite sphere, a single sphere with the electromagnetic field frequency of 10 GHz is selected to investigate the micro-electromagnetic distribution and loss characteristics. By carefully comparing the loss characteristics of different layers of spheres, the absorption characteristics of composite spheres at different positions are the same, so the distribution of energy loss is also the same. On the other hand, considering the fact that with the consumption of electromagnetic energy in the propagation process, the top sphere is closer to the electromagnetic emission port, and its energy loss intensity is slightly greater than that of the bottom sphere, so we select layer 34 sphere as the representative of the numerical model. Fig. 4a presents the Poynting vector of the electromagnetic field around the micro-sphere and the electric field intensity of the composite sphere. The thickness of the arrow represents the magnitude of the Poynting vector. The results show that the propagation of the electromagnetic field is largely affected by the spherical structure, and the electric field intensity increases at the contact points between the spheres. Especially at the contact point where the tangent plane of the contact point is perpendicular to the direction of the electric field, and the enhancement of the electric field is most obvious. When the wave length is larger than the size of the sphere, the electromagnetic field shows the characteristics of electrostatic field, so the electrostatic concentration effect appears at the contact position of the sphere.

Considering that the graphene is a typical electrical loss material, the electric field loss in the graphene layer is much greater than that in the FeCo core. Besides, the electric field loss at the concentration point in the graphene layer is much greater than that in other places (Fig. 4b). As a magnetic loss medium, the loss of magnetic field is mainly produced by the FeCo core, as shown in Fig. 4c. Based on the results shown in Fig. 4b and c, we can see that the loss density of the electric field in the graphene layer is far greater than that in the FeCo core magnetic field. Hence, the coating of the graphene layer can increase the electric field loss, thus improving the microwave absorbing performance of the whole material.

In addition, the effect of the thickness of the graphene layer encapsulating the FeCo alloy on the microwave absorption performance has been investigated. The thickness of the graphene layer is increased to 0.4 times of the radius of the composite sphere. Compared with the results of single graphene layer, the most important change is that the overall reflection coefficient of sphere arrangement increases for the multilayer coating (Fig. 4d). As a good conductive medium, graphene has a strong electromagnetic shielding ability. As shown in Fig. 4d, too thick graphene shell can enhance the reflected electromagnetic field, which will reduce the electromagnetic intensity into the particle, thus reducing the microwave absorption performance of the whole composite. The loss characteristics of a multilayer graphene encapsulating FeCo sphere at the same position and electromagnetic frequency as shown in

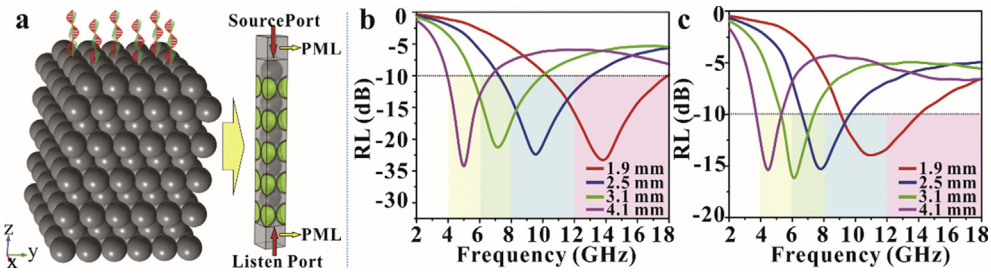

Fig. 3. The geometry of the numerical model and the energy loss curve based on the simulated numerical models. (a) The geometry of the numerical model; (b) the simulated reflection loss of FeCo alloy encapsulated by single layer graphene; and (c) the simulated reflection loss of FeCo alloy encapsulated by multilayer graphene.

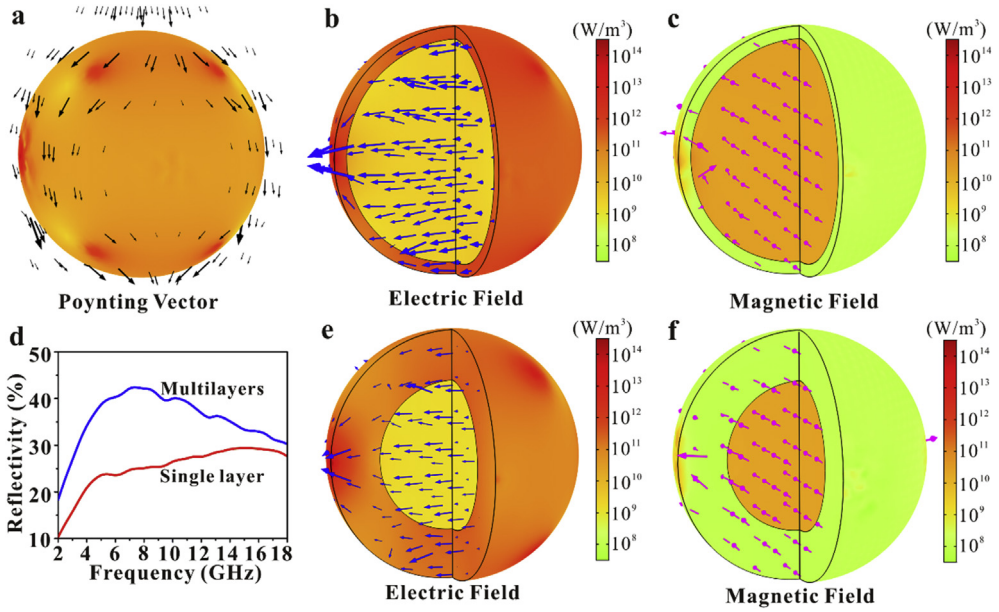

Fig. 4. The micro-electromagnetic distribution and loss characteristics of the numerical models. (a) The Poynting vector of the electromagnetic field around the micro-sphere and the electric field intensity of the composite sphere; (b) the electric field loss and electric field vector of single layer graphene encapsulating FeCo sphere; (c) the magnetic field loss and magnetic field vector of single layer graphene encapsulating FeCo sphere; (d) the reflection coefficients of single layer graphene and multilayer graphene encapsulating FeCo spheres; (e) the electric field loss and electric field vector of multilayer graphene encapsulating FeCo sphere; and (f) the magnetic field loss and magnetic field vector of multilayer graphene encapsulating FeCo sphere. The thickness of the arrow represents the size of the electromagnetic vector.

Fig. 4a are given in Fig. 4e and f. As the emission coefficient increases, the intensity of the electromagnetic field entering the sphere decreases. The magnitude of the electric field vector in Fig. 4e is significantly smaller than that in Fig. 4b. Therefore, as the thickness of the graphene layer increases, the range of electric field loss increases, while the intensity of electric field loss decreases. Compared with the results in Fig. 4c and f, we can see that the range and intensity of the magnetic field loss are both reduced in the FeCo core. Hence, decreasing the coating thickness to single layer graphene can render a good match between the electric field and the magnetic field, and thus resulting in an electrifying microwave absorption performance. It should be pointed out that the single layer graphene coating not only protects the magnetic metal core with strong magnetic loss but also makes full use of the strong electric field characteristics of the contact point, resulting in strong electrical loss. Without the graphene layer coating, the electric field loss of the bare FeCo particle is reduced greatly (Fig. S13), which will also reduce the microwave absorption performance of FeCo particles.

Consequently, the essential factors that result in FeCo@Cs with good microwave absorption performance can be concluded as below: (1) the graphene shell can avoid the oxidation of FeCo core and ensure the magnetic loss ability of the composites; (2) the contact position of spherical particles will produce a strong electric field, and the introduction of single layer graphene coating takes advantage of the strong electric loss characteristics of graphene, resulting in a large energy loss at the electric field enhancement point; and (3) the core@shell structures increase the electromagnetic surface via abundant multiple interfaces among the composites, such as graphene shell/graphene shell and magnetic core/graphene, which will also favor the microwave absorption property.

3. Conclusions

In summary, using the channels of ordered mesoporous silica as template, single layer graphene encapsulating FeCo alloy nanoparticles were successfully prepared via a CVD-assisted strategy. The prepared sample shows excellent microwave absorption performance. The strongest RL values can reach −46 dB, by varying the simulation thickness, and the RL values of the sample can exceed −10 dB in the whole Ku-band (1.8–2.1 mm), whole X-band (2.5 mm), whole C2-band (3.1 mm), and even in the whole C1-band (4.5 mm). The enhanced microwave absorption performance of FeCo@Cs can be attributed to the synergistic effect of single layer graphene coating and FeCo alloy cores. Besides avoiding oxidation of FeCo alloy cores, the numerical simulation results show that the introduction of the single layer graphene can improve the absorbing performance greatly by increasing the dielectric loss. It is also demonstrated that the increase in graphene layer thickness will increase the reflected electromagnetic field and reduce the absorbing performance. Our results give new insights into the absorption enhancement of magnetic metal@C nanostructures and contribute to guide the design and development of highly efficient microwave absorption materials for practical application.

4. Experimental section

Single layer graphene encapsulating FeCo alloy nanoparticles (FeCo@Cs) were prepared through CVD method. First, $Fe(NO_3)_3 \cdot 9H_2O$ (1.8 mmol) and $Co(NO_3)_2 \cdot 6H_2O$ (1.8 mmol) were filled into the channel of SBA-15 by an impregnation method in methanol solution, named as FeCo@SBA-15. Then the deposits were transferred into a CVD furnace, temperature programmed from room temperature to 800 °C under 50% H_2/Ar, followed by CH_4 for 5 min at 800 °C. Finally, the samples were treated in 4% HF aqueous solution at room temperature for 4 h, followed by washing in distilled water and ethanol, and drying at 80 °C for 12 h.

The morphology and microstructures of the products were investigated using TEM (FEI Tecnai F20, 200 kV). Elemental mapping images were performed with an energy dispersive X-ray detector (EDX) system attached to TEM. The XRD was performed on a Rigaku D/Max-2500 diffractometer with Cu Kα radiation. XPS was

measured on a Perkin-Elmer model PHI 5600 XPS system from a monochromatic aluminum anode X-ray source with Kα radiation. The effective complex permittivity and permeability were measured using an Agilent 85071E vector network analyzer in the frequency range of 2–18 GHz. The RL values were calculated according to transmission line theory.

The numerical simulation was performed in the software of COMSOL multiphysics. In the numerical model (Fig. 3a), large-size simulated particles are used to replace multiple nano-scale real particles with the same amount of matter. PMLs on the top and bottom of the computational domain are used to absorb the electromagnetic field from the ports. And Floquet-periodic boundary conditions are carried out to extend the array structure infinitely. The electromagnetic parameters of FeCo core are obtained by inverse solution of experimental results.

Credit author statement

X.J. Cui, Q.R. Jiang: Investigation, Validation, Data curation, Visualization, Writing – Original draft preparation. **C.S. Wang**: Software, Methodology, Data Curation, Visualization, Writing – Original draft preparation. **S.H. Wang**: Validation, Data curation, Visualization. **Z.Y. Jiang**: Conceptualization, Supervision, Resources, Funding acquisition, Writing – Review & Editing. **X.A. Li**: Project administration, Resources, Funding acquisition, Writing – Review & Editing. **D.H. Deng**: Supervision, Resources, Funding acquisition, Writing – Review & Editing.

Declaration of competing interest

The authors declare that they have no known competing financial interests or personal relationships that could have appeared to influence the work reported in this paper.

Acknowledgments

This work was supported by the National Natural Science Foundation of China (No. 51802278, 21988101, 21771151, 21890753, and 21931009), the National Key R&D Program of China (No. 2016YFA0204100), the Strategic Priority Research Program of Chinese Academy of Sciences (No. XDB36030200), and the Key Research Program of Frontier Sciences of the Chinese Academy of Sciences (No. QYZDB-SSW-JSC020).

Appendix A. Supplementary data

Supplementary data to this article can be found online at https://doi.org/10.1016/j.mtnano.2021.100138.

References

[1] Y. Ra'di, C.R. Simovski, S.A. Tretyakov, Thin perfect absorbers for electromagnetic waves: theory, design, and realizations, Phys. Rev. Appl. 3 (2015), 037001.
[2] R.C. Che, L.M. Peng, X.F. Duan, Q. Chen, X.L. Liang, Microwave absorption enhancement and complex permittivity and permeability of Fe encapsulated within carbon nanotubes, Adv. Mater. 16 (2004) 401–405.
[3] F. Wang, C. Bai, L. Chen, Y. Yu, Boron nitride nanocomposites for microwave absorption: a review, Mater. Today Nano 13 (2021) 100108.
[4] Y. Zhang, Y. Huang, T.F. Zhang, H.C. Chang, P.S. Xiao, H.H. Chen, Z.Y. Huang, Y.S. Chen, Broadband and tunable high-performance microwave absorption of an ultralight and highly compressible graphene foam, Adv. Mater. 27 (2015) 2049–2053.
[5] B. Wen, X.X. Wang, W.Q. Cao, H.L. Shi, M.M. Lu, G. Wang, H.B. Jin, W.Z. Wang, J. Yuan, M.S. Cao, Reduced graphene oxides: the thinnest and most lightweight materials with highly efficient microwave attenuation performances of the carbon world, Nanoscale 6 (2014) 5754–5761.
[6] M. Green, L.H. Tian, P. Xiang, J. Murowchick, X.Y. Tan, X.B. Chen, Co_2P nanoparticles for microwave absorption, Mater. Today Nano 1 (2018) 1–7.
[7] M. Qin, L.M. Zhang, X.R. Zhao, H.J. Wu, Defect induced polarization loss in multi-shelled spinel hollow spheres for electromagnetic wave absorption application, Adv. Sci. 8 (2021) 2004640.
[8] Q.H. Liu, Q. Cao, H. Bi, C.Y. Liang, K.P. Yuan, W. She, Y.J. Yang, R.C. Che, CoNi@SiO_2 @TiO_2 and CoNi@Air@TiO_2 microspheres with strong wideband microwave absorption, Adv. Mater. 28 (2016) 486–490.
[9] Y.J. Huang, J. Luo, M.B. Pu, Y.H. Guo, Z.Y. Zhao, X.L. Ma, X. Li, X.G. Luo, Catenary electromagnetics for ultra-broadband lightweight absorbers and large-scale flat antennas, Adv. Sci. 6 (2019) 1801691.
[10] Q. Long, Z.Q. Xu, H.H. Xiao, K.N. Xie, A facile synthesis of a cobalt nanoparticle–graphene nanocomposite with high-performance and triple-band electromagnetic wave absorption properties, RSC Adv. 8 (2018) 1210–1217.
[11] B. Bateer, Y. Xie, C.G. Tian, W.X. Ping, Cobalt nanoparticles decorated on nitrogen-doped graphene as excellent electromagnetic wave absorbent in Ku-band, J. Mater. Sci. Mater. Electron. 31 (2020) 12044–12055.
[12] D.F. Zhang, Y.F. Deng, C.A. Han, H.P. Zhu, C.J. Yan, H.Y. Zhang, Enhanced microwave absorption bandwidth in graphene-encapsulated iron nanoparticles with core-shell structure, Nanomaterials 10 (2020) 931.
[13] Q. Yu, Y.Y. Wang, P. Chen, H.L. Chen, W.C. Nie, Y.Q. Liu, Graphene anchored with super-tiny Ni nanoparticles for high performance electromagnetic absorption applications, J. Mater. Sci. Mater. Electron. 30 (2019) 14480–14489.
[14] B. Wen, M.S. Cao, M.M. Lu, W.Q. Cao, H.L. Shi, J. Liu, X.X. Wang, H.B. Jin, X.Y. Fang, W.Z. Wang, J. Yuan, Reduced graphene oxides: light-weight and high-efficiency electromagnetic interference shielding at elevated temperatures, Adv. Mater. 26 (2014) 3484–3489.
[15] A. Iqbal, F. Shahzad, K. Hantanasirisakul, M.K. Kim, J. Kwon, J. Hong, H. Kim, D. Kim, Y. Gogotsi, C.M. Koo, Anomalous absorption of electromagnetic waves by 2D transition metal carbonitride Ti_3CNT_x (MXene), Science 369 (2020) 446–450.
[16] X.X. Wang, W.Q. Cao, M.S. Cao, J. Yuan, Assembling nano–microarchitecture for electromagnetic absorbers and smart devices, Adv. Mater. 32 (2020) 2002112.
[17] F. Shahzad, M. Alhabeb, C.B. Hatter, B. Anasori, S.M. Hong, C.M. Koo, Y. Gogotsi, Electromagnetic interference shielding with 2D transition metal carbides (MXenes), Science 353 (2016) 1137–1140.
[18] Z.H. Zeng, C.X. Wang, G. Siqueira, D.X. Han, A. Huch, S. Abdolhosseinzadeh, J. Heier, F. Nüesch, C.F. Zhang, G. Nyström, Nanocellulose-MXene biomimetic aerogels with orientation-tunable electromagnetic interference shielding performance, Adv. Sci. 7 (2020) 2000979.
[19] L.Y. Liang, Z.Y. Li, Z.Y. Bai, Y.Z. Feng, X.Q. Guo, J.M. Ma, C.T. Liu, Dependence of electromagnetic wave absorption properties on the topography of Ni anchoring on reduced graphene oxide, Chin. Chem. Lett. 32 (2021) 870–874.
[20] H.H. Chen, Z.Y. Huang, Y. Huang, Y. Zhang, Z. Ge, W.L. Ma, T.F. Zhang, M.M. Wu, S.T. Xu, F. Fan, S.J. Chang, Y.S. Chen, Consecutively strong absorption from gigahertz to terahertz bands of a monolithic three-dimensional Fe_3O_4/graphene material, ACS Appl. Mater. Interfaces 11 (2019) 1274–1282.
[21] Z.C. Wu, K. Pei, L.S. Xing, X.F. Yu, W.B. You, R.C. Che, Enhanced microwave absorption performance from magnetic coupling of magnetic nanoparticles suspended within hierarchically tubular composite, Adv. Funct. Mater. 29 (2019) 1901448.
[22] Y.L. Ren, H.Y. Wu, M.M. Lu, Y.J. Chen, C.L. Zhu, P. Gao, M.S. Cao, C.Y. Li, Q.Y. Ouyang, Quaternary nanocomposites consisting of graphene, Fe_3O_4@FeCore@shell, and ZnO nanoparticles: synthesis and excellent electromagnetic absorption properties, ACS Appl. Mater. Interfaces 4 (2012) 6436–6442.
[23] H.B. Zhao, J.B. Cheng, J.Y. Zhu, Y.Z. Wang, Ultralight CoNi/rGO aerogels toward excellent microwave absorption at ultrathin thickness, J. Mater. Chem. C 7 (2019) 441–448.
[24] G.B. Sun, H. Wu, Q.L. Liao, Y. Zhang, Enhanced microwave absorption performance of highly dispersed CoNi nanostructures arrayed on graphene, Nano Res 11 (2018) 2689–2704.
[25] X.F. Zhang, X.L. Dong, H. Huang, Y.Y. Liu, W.N. Wang, X.G. Zhu, B. Lv, J.P. Lei, C.G. Lee, Microwave absorption properties of the carbon-coated nickel nanocapsules, Appl. Phys. Lett. 89 (2006), 053115.
[26] T.T. Chen, F. Deng, J. Zhu, C.F. Chen, G.B. Sun, S.L. Ma, X.J. Yang, Hexagonal and cubic Ni nanocrystals grown on graphene: phase-controlled synthesis, characterization and their enhanced microwave absorption properties, J. Mater. Chem. 22 (2012) 15190–15197.
[27] Z.T. Zhu, X. Sun, G.X. Li, H.R. Xue, H. Guo, X.L. Fan, X.C. Pan, J.P. He, Microwave-assisted synthesis of graphene–Ni composites with enhanced microwave absorption properties inKu-band, J. Magn. Magn. Mater. 377 (2015) 95–103.
[28] G.H. Pan, J. Zhu, S.L. Ma, G.B. Sun, X.J. Yang, Enhancing the electromagnetic performance of Co through the phase-controlled synthesis of hexagonal and cubic Co nanocrystals grown on graphene, ACS Appl. Mater. Interfaces 5 (2013) 12716–12724.
[29] H.L. Lv, G.B. Ji, X.H. Liang, H.Q. Zhang, Y.W. Du, A novel rod-like MnO_2@Fe loading on graphene giving excellent electromagnetic absorption properties, J. Mater. Chem. C 3 (2015) 5056–5064.
[30] X.F. Xu, S.H. Shi, Y.L. Tang, G.Z. Wang, M.F. Zhou, G.Q. Zhao, X.C. Zhou, S.W. Lin, F.B. Meng, Growth of NiAl-layered double hydroxide on graphene toward excellent anticorrosive microwave absorption application, Adv. Sci. 8 (2021) 2002658.
[31] X.S. Qi, Q. Hu, H.B. Cai, R. Xie, Z.C. Bai, Y. Jiang, S.J. Qin, W. Zhong, Y.W. Du, Heteronanostructured Co@carbon nanotubes-graphene ternary hybrids: synthesis, electromagnetic and excellent microwave absorption properties, Sci. Rep. 6 (2016) 37972.

[32] H. Wang, H.H. Guo, Y.Y. Dai, D.Y. Geng, Z. Han, D. Li, T. Yang, S. Ma, W. Liu, Z.D. Zhang, Optimal electromagnetic-wave absorption by enhanced dipole polarization in Ni/C nanocapsules, Appl. Phys. Lett. 101 (2012), 083116.
[33] H. Wang, Y.Y. Dai, W.J. Gong, D.Y. Geng, S. Ma, D. Li, W. Liu, Z.D. Zhang, Broadband microwave absorption of CoNi@C nanocapsules enhanced by dual dielectric relaxation and multiple magnetic resonances, Appl. Phys. Lett. 102 (2013) 223113.
[34] H. Wang, Y.Y. Dai, D.Y. Geng, S. Ma, D. Li, J. An, J. He, W. Liu, Z.D. Zhang, Co_xNi_{100-x} nanoparticles encapsulated by curved graphite layers: controlled in situ metal-catalytic preparation and broadband microwave absorption, Nanoscale 7 (2015) 17312–17319.
[35] X.C. Zhao, Z.M. Zhang, L.Y. Wang, K. Xi, Q.Q. Cao, D.H. Wang, Y. Yang, Y.W. Du, Excellent microwave absorption property of graphene-coated Fe nanocomposites, Sci. Rep. 3 (2013), 03421.
[36] X.G. Liu, B. Li, D.Y. Geng, W.B. Cui, F. Yang, Z.G. Xie, D.J. Kang, Z.D. Zhang, (Fe, Ni)/C nanocapsules for electromagnetic-wave-absorber in the whole Ku-band, Carbon 47 (2009) 470–474.
[37] H. Li, S.S. Bao, Y.M. Li, Y.Q. Huang, J.Y. Chen, H. Zhao, Z.Y. Jiang, Q. Kuang, Z.X. Xie, Optimizing the electromagnetic wave absorption performances of designed Co_3Fe_7@C yolk–shell structures, ACS Appl. Mater. Interfaces 10 (2018) 28839–28849.
[38] P.B. Liu, S. Gao, G.Z. Zhang, Y. Huang, W.B. You, R.C. Che, Hollow engineering to Co@N-doped carbon nanocages via synergistic protecting-etching strategy for ultrahigh microwave absorption, Adv. Funct. Mater. 31 (2021) 2102812.
[39] S. Gao, G.Z. Zhang, Y. Wang, X.P. Han, Y. Huang, P.B. Liu, MOFs derived magnetic porous carbon microspheres constructed by core-shell Ni@C with high-performance microwave absorption, J. Mater. Sci. Technol. 88 (2021) 56–65.
[40] X.L. Dong, X.F. Zhang, H. Huang, F. Zuo, Enhanced microwave absorption in Ni/polyaniline nanocomposites by dual dielectric relaxations, Appl. Phys. Lett. 92 (2008), 013127.
[41] X.J. Cui, P.J. Ren, D.H. Deng, J. Deng, X.H. Bao, Single layer graphene encapsulating non-precious metals as high-performance electrocatalysts for water oxidation, Energy Environ. Sci. 9 (2016) 123–129.
[42] A.C. Ferrari, J.C. Meyer, V. Scardaci, C. Casiraghi, M. Lazzeri, F. Mauri, S. Piscanec, D. Jiang, K.S. Novoselov, S. Roth, A.K. Geim, Raman spectrum of graphene and graphene layers, Phys. Rev. Lett. 97 (2006) 187401.
[43] Z.R. Jia, D. Lan, K.J. Lin, M. Qin, K.C. Kou, G.L. Wu, H.J. Wu, Progress in low-frequency microwave absorbing materials, J. Mater. Sci. Mater. Electron. 29 (2018) 17122–17136.
[44] N. Gill, S. Puthucheri, D. Singh, V. Agarwala, Critical analysis of frequency selective surfaces embedded composite microwave absorber for frequency range 2-8 GHz, J. Mater. Sci. Mater. Electron. 28 (2017) 1259–1270.
[45] T. Guo, B. Huang, C.G. Li, Y.M. Lou, X.Z. Tang, X.Z. Huang, J.L. Yue, Magnetic sputtering of FeNi/C bilayer film on SiC fibers for effective microwave absorption in the low-frequency region, Ceram. Int. 47 (2021) 5221–5226.
[46] H.L. Peng, X. Zhang, H.L. Yang, Z.Q. Xiong, C.B. Liu, Y. Xie, Fabrication of core-shell nanoporous carbon@chiral polyschiff base iron(II) composites for high-performance electromagnetic wave attenuation in the low-frequency, J. Alloy. Compd. 850 (2021) 156816.
[47] B. Quan, X.H. Liang, G.B. Ji, Y.N. Zhang, G.Y. Xu, Y.W. Du, Cross-linking-derived synthesis of porous Co_xNi_y/C nanocomposites for excellent electromagnetic behaviors, ACS Appl. Mater. Interfaces 9 (2017) 38814–38823.
[48] D. Ding, Y. Wang, X.D. Li, R. Qiang, P. Xu, W.L. Chu, X.J. Han, Y.C. Du, Rational design of core-shell Co@C microspheres for high-performance microwave absorption, Carbon 111 (2017) 722–732.
[49] X.X. Xie, H. Wang, Y.P. Zhou, K.M. Huang, One-step self-triggered microwave-assisted fabrication of NiCo graphene for microwave attenuation, J. Mater. Sci. Mater. Electron. 31 (2020) 12467–12475.
[50] Z.Y. Bai, X.Q. Guo, L. Fan, K. Gao, J.W. Liu, W.Z. Song, Y. Li, R. Zhang, Synergism of 1D CoNi chains anchored 2D reduced graphene oxide with strong interfacial interactions to enhance microwave absorption properties, J. Mater. Sci. Mater. Electron. 30 (2019) 3792–3803.
[51] H.X. Zhang, C. Shi, Z.R. Jia, X.H. Liu, B.H. Xu, D.D. Zhang, G.L. Wu, FeNi nanoparticles embedded reduced graphene/nitrogen-doped carbon composites towards the ultra-wideband electromagnetic wave absorption, J. Colloid Interface Sci. 584 (2021) 382–394.
[52] J. Li, D. Zhang, H. Qi, G.M. Wang, J.M. Tang, G. Tian, A.H. Liu, H.J. Yue, Y. Yue, S.H. Feng, Economical synthesis of composites of FeNi alloy nanoparticles evenly dispersed in two-dimensional reduced graphene oxide as thin and effective electromagnetic wave absorbers, RSC Adv. 8 (2018) 8393–8401.
[53] D. An, Z.Y. Zhang, Y.H. Wang, S.S. Cheng, Y.Q. Liu, The distinctly enhanced electromagnetic wave absorption properties of FeNi/rGO nanocomposites compared with pure FeNi alloys, J. Supercond. Nov. Magn. 32 (2019) 385–392.
[54] G. Demésy, F. Zolla, A. Nicolet, M. Commandré, Versatile full-vectorial finite element model for crossed gratings, Opt. Lett. 34 (2009) 2216–2218.